Electrophoretic deposition of iron oxide nanoparticles to achieve thick nickel/iron oxide magnetic nanocomposite films

Cite as: AIP Advances **10**, 015308 (2020); https://doi.org/10.1063/1.5129797
Submitted: 01 October 2019 . Accepted: 02 December 2019 . Published Online: 07 January 2020

Sara C. Mills, Connor S. Smith, David P. Arnold, and Jennifer S. Andrew

Electrophoretic deposition of iron oxide nanoparticles to achieve thick nickel/iron oxide magnetic nanocomposite films

Cite as: AIP Advances 10, 015308 (2020); doi: 10.1063/1.5129797
Presented: 5 November 2019 • Submitted: 1 October 2019 •
Accepted: 2 December 2019 • Published Online: 7 January 2020

Sara C. Mills,[1] Connor S. Smith,[2] David P. Arnold,[2] and Jennifer S. Andrew[1,a)]

AFFILIATIONS

[1] Department of Materials Science and Engineering, University of Florida, Gainesville, Florida 32611-6400, USA
[2] Department of Electrical and Computer Engineering, University of Florida, Gainesville, Florida 32611-6200, USA

Note: This paper was presented at the 64th Annual Conference on Magnetism and Magnetic Materials.
[a)] **Electronic mail:** jandrew@mse.ufl.edu

ABSTRACT

For modern switching power supplies, current bulk magnetic materials, such as ferrites or magnetic metal alloys, cannot provide both low loss and high magnetic saturation to function with both high power density and high efficiency at high frequencies (10-100 MHz). Magnetic nanocomposites comprised of a ferrite and magnetic metal alloy provide the opportunity to achieve these desired magnetic properties, but previously investigated thin-film fabrication techniques have difficulty achieving multi-micrometer film thicknesses which are necessary to provide practical magnetic energy storage and power handling. Here, we present a versatile technique to fabricate thick magnetic nanocomposites via a two-step process, consisting of the electrophoretic deposition of an iron oxide nanoparticle phase into a mold on a substrate, followed by electro-infiltration of a nickel matrix. The deposited films are imaged via scanning electron microscopy and energy dispersive X-ray spectroscopy to identify the presence of iron and nickel, confirming the infiltration of the nickel between the iron oxide nanoparticles. A film thickness of ~7 μm was measured via stylus profilometry. Further confirmation of successful composite formation is obtained with vibrating sample magnetometry, showing the saturation magnetization value of the composite (473 kA/m) falls between that of the iron oxide nanoparticles (280 kA/m) and the nickel matrix (555 kA/m). These results demonstrate the potential of electrophoretic deposition coupled with electro-infiltration to fabricate magnetic nanocomposite films.

I. INTRODUCTION

As electronic devices continue to be miniaturized there is a corresponding need for smaller on-chip power converters, and it is also necessary to ensure that performance does not suffer as the size of the underlying power components decreases.[1] Many of the current magnetic materials used for these power components are single phase materials, such as ferrites or magnetic metal alloys.[2] At high frequency operation, eddy current losses become significant and higher permeability materials such as magnetic metal alloys result in less efficient components.[1,3,4] To retain high magnetic saturation and permeability but incorporate the low loss of ferrites, magnetic nanocomposites show promise for producing materials with these desired magnetic properties. Recent work has demonstrated that magnetic nanocomposites composed of two magnetic materials have the ability to exhibit the desired magnetic properties, thus satisfying the need for a magnetic material with both low loss and high magnetic saturation.[5,6]

The fabrication of films of ferrites and/or magnetic metal alloys for magnetic nanocomposites have included vacuum techniques such as sputtering single or multiple layers, screen printing, and drop-casting.[1,6,7] To provide improved magnetic energy storage and power handling, thick (tens of micrometers) nanocomposites are needed.[2] Deposition methods such as sputtering have the ability to achieve complex compositions, but cannot economically produce thick final composites.[8] A more economical approach, such as

drop-casting, could be more palatable for the assembly of thicker films of nanoparticles, but can lead to non-uniform and uncontrollable film thickness.[9]

One method of depositing thick films of nanoparticles for a composite in a cost-effective manner and relatively short amount of time is electrophoretic deposition (EPD).[10] EPD (Figure 1a) is a process in which a colloidal solution of charged particles, typically in a non-aqueous solution, are deposited onto a conductive substrate under the application of a DC electric field. In addition to being cost-effective, EPD has been used to deposit thick, porous films, some of which exceed 100 μm thick with a variety of ceramic materials such as alumina, magnesia, and yttria stabilized zirconia.[11] The deposition of magnetic nanoparticles via EPD, however, has also been accomplished, but much less frequently.[12–14]

Electrophoretic deposition can then be adapted as a method to fabricate thick magnetic nanocomposites composed of a magnetic nanoparticle inclusion phase followed by electro-infiltration of a magnetic metal alloy. Electro-infiltration, a process that electroplates a magnetic metal through a porous layer of nanoparticles, has been explored for use in these kinds of applications, but the deposition of the magnetic nanoparticle films have exclusively been accomplished via drop-casting.[5,6,15,16]

This work describes the use of EPD for the assembly of iron oxide nanoparticles into a mold. Nickel is then electro-infiltrated into the iron oxide nanoparticle film, where the electroplating fills the pores between the particles with metal. By using a low loss magnetic phase (e.g., iron oxide nanoparticles) and a high magnetic saturation phase (e.g., nickel), this work demonstrates the potential of EPD coupled with electro-infiltration for the fabrication of these magnetic nanocomposite films for on-chip power components. This method of coupilng EPD with electroinfiltration presents a versatile tool to fabricate a wide range of nanoparticle-based composites for functional applications.

II. EXPERIMENTAL

A. Nanoparticle synthesis

Iron oxide nanoparticles were synthesized via aqueous co-precipitation by the addition of iron (II) and iron (III) chloride salts in a molar ratio of 1:2, respectively. These salts were reacted in alkaline (pH 8-9) conditions for one hour at 85°C. After synthesis, the resulting particles were collected with a large permanent magnet, washed, and dialyzed for the removal of any excess salts. After dialysis, the particles were collected and re-suspended in water with the addition of tetraethylammonium hydroxide (TEAH). TEAH acted as a peptizing agent to create a colloidally stable solution of nanoparticles in water to serve as a stock solution. This synthesis was done with reference to a previously reported method.[17]

B. Magnetic nanocomposite fabrication

A comprehensive overview of the entire fabrication process can be seen in Figure 1b. This process is comprised of four steps: 1) patterning of the substrates into 5 mm diameter circular molds, 2) electrophoretic deposition of iron oxide nanoparticles, 3) electro-infiltration of nickel between the iron oxide nanoparticles, 4) and lastly mold removal with acetone.

1. Substrate patterning

The substrate was a (100) p-type silicon wafer with a 10 nm titanium adhesion layer, upon which a 100 nm gold seed layer was DC-sputtered onto it using KJL CMS-18 Multi-Source sputtering tool. The substrate was then treated with an HDMS vapor primer and patterned into an array of 5 mm diameter circular molds using a 10 μm layer of KMPR 1010 negative photoresist. After a 5 minute softbake at 100°C, an exposure dose of 670 mJ/cm^2 was applied. A post-exposure bake of 2 minutes at 100°C was then applied, followed by a 2 minute development time in 1-methoxy-2-propanol acetate. The patterned sample was then rinsed with isopropanol and DI water and blown dry with nitrogen.

2. Electrophoretic deposition

Iron oxide nanoparticles from the stock solution were added at one volume percent (1 vol %) to a solution of 0.01 M hydrochloric acid (HCl) in isopropanol (IPA), providing the particles with a positive surface charge, with a measured positive zeta potential of ~30 mV. The zeta potential of the particles was measured with a dilute solution of the nanoparticles in water by using a Brookhaven ZetaPlus instrument. This solution of positively charged particles

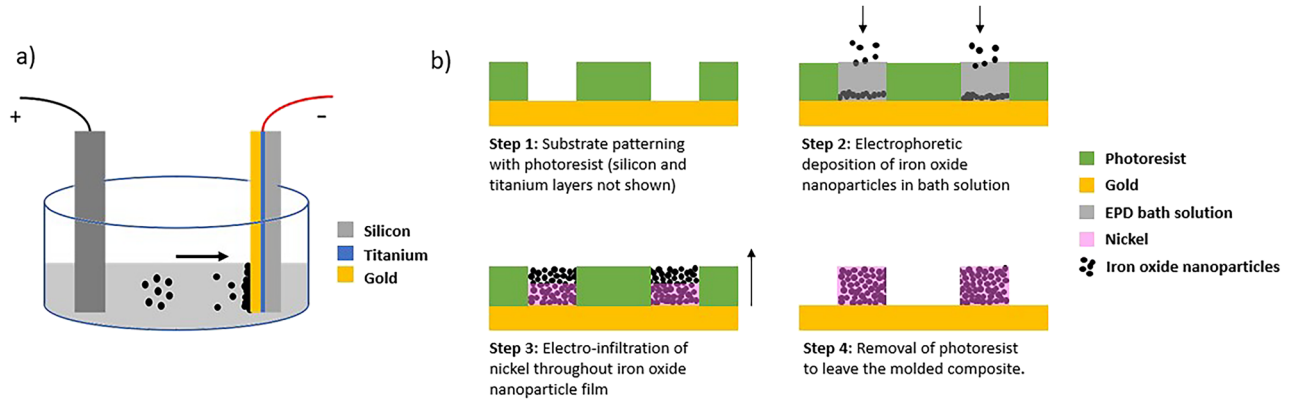

FIG. 1. (a) Schematic of electrophoretic deposition (EPD) with a graphite block as the positive electrode and the substrate as the negative electrode. (b) Overview of the nanocomposite fabrication process.

could then move towards a negatively charged electrode, or substrate, under an externally applied electric field. In this case, the particles deposited onto the patterned silicon substrates. The positively charged electrode consisted of a graphite block, acting as the counter electrode, placed parallel to the substrate. The set-up for this process can be seen in Figure 1a. The counter electrode and substrates were placed 1.5 cm apart, a field of 30 V/cm was applied, and EPD was carried out for 45 minutes. After EPD, the films were allowed to dry overnight prior to nanocomposite fabrication via electro-infiltration.

3. Electro-infiltration

After deposition of the ferrite nanoparticles onto the patterned substrate, an electro-infiltration method was used to form the final magnetic nanocomposite. Electro-infiltration is a techinque where a metal is electroplated through a nanoparticle film to fill the spaces between the nanoparticles.[15] For these samples, a nickel sulfamate bath from Technic Inc. (Technic Nickel "S") was used, with a 5x5 cm^2 nickel foil used as the anode and the substrate used as the cathode. To ensure the magnetic nanoparticles were held in place a 1 cm^3 cube-shaped neodynium-iron-boron (NdFeB) retaining magnet was placed behind the substrate. Plating was then performed at 54°C with agitation from a magnetic stir bar spinning at 60 rpm and a current density of 10 mA/cm^2 for ~20 minutes. After plating, the samples were rinsed with DI water and dried with nitrogen, and the photoresist mold was subsequently removed using acetone.

C. Characterization

The crystalline phase of the synthesized iron oxide nanoparticles was confirmed with X-ray diffraction (XRD) using a Panalytical X'pert powder diffractometer. This instrument used a Cu anode to supply Kα radiation and a scintillation detector (45 kV, 40 mA). Iron oxide nanoparticle samples were analyzed with a step size of 0.016°. The phase was confirmed with comparison to a magnetite (Fe_3O_4) reference pattern 98-004-4525 from the International Center for Diffraction Data (ICDD) database. Scherrer's formula was used to calculate the crystallite size of the particles. Briefly, Scherrer's formula, $\tau = \frac{k\lambda}{\beta cos\theta}$, is used to calculate the crystallite size (τ), where k is a shape factor (assumed to be 0.9 for spherical particles), λ is the X-ray wavelength (1.54 Å), β is the full width half maximum value (corrected for instrument broadening) in radians, and θ is the Bragg angle, also in radians.

Magnetic characterization of the iron oxide nanoparticles, electroplated nickel film, and magnetic nanocomposites was done with an ADE Tech. EV-9 vibrating sample magnetometer. Magnetic fields between -1800 and 1800 kA/m were applied at room temperature.

The physical size of the iron oxide nanoparticles was characterized using images obtained with a 100 kV Hitachi H7000 TEM. A dilute solution of particles from the stock solution was placed on a formvar-coated Cu mesh grid for imaging. ImageJ software from the NIH was used for size measurements (n=250).

The thickness of the nanocomposites was measured with a Tencor Alpha-Step AS500 stylus profilometer. Profilometry was performed on nanocomposites after the photoresist was removed.

To confirm magnetic nanocomposite formation, cross sections of the magnetic nanocomposites were analyzed with scanning electron microscopy (SEM). This was accomplished with an FEI Nova NanoSEM 430 at an accelerating voltage of 15 keV at a working distance of 5.3 mm. Energy dispersive X-ray spectroscopy (EDS) capabilities on the FEI Nova NanoSEM were utilized to identify detectable concentrations of the elements of iron and nickel. If present and well-dispersed, this confirms the successful infiltration of nickel within the iron oxide nanoparticle matrix.

III. RESULTS AND DISCUSSION

A. Nanoparticles

An X-ray diffraction (XRD) pattern of the as synthesized nanoparticles is shown in Figure 2a. The synthesized iron oxide nanoparticles were compared to a magnetite (Fe_3O_4) reference pattern 98-004-4525 from the ICCD database. The peaks seen at 2θ = 30.1, 35.4, 53.4, 56.9, and 62.5° are indicative of a inverse spinel crystal structure, which was expected from this phase of iron oxide. To calculate crystallite size, Scherrer's formula was used and three peaks at the following 2θ values were chosen for the calculations: 35.7, 57.6, and 63.2°. The average crystallite size was calculated as 10.3 ± 1.3 nm. In comparison, the physical size, measured by using images from transmission electron microscopy (TEM), was measured at 10.6 ± 2.4 nm (Figure 2b).

Vibrating sample magnetometry (VSM) was used to probe the out-of-plane magnetic behavior of the iron oxide nanoparticles at room temperature. The hysteresis curve of a film of these particles (found in Figure 3a) shows a magnetic saturation (M_s) value of 280 kA/m and a coercivity (H_c) of 0.26 kA/m. In comparison to the bulk M_s of magnetite, 476 kA/m, this nanoparticle film achieved approximately 59% of the bulk value. This can be attributed to the porosity of the film and the inherently lower magnetic saturation of nanoparticles as compared to the bulk. The low coercivity of the nanoparticle film, 0.26 kA/m, is larger than expected of particles of this physical size, which should be superparamagnetic and exhibit no coercivity. However, this coercivity value arises due to particle-particle interactions in the sample.[18] XRD shows that inverse spinel iron oxide nanoparticles were synthesized, with VSM confirming the magnetic behavior of particles that satisfy the material properties for a low loss ferrite inclusion phase.

B. Magnetic nanocomposites

The magnetic nanocomposites which were fabricated as illustrated in Figure 1b were cleaved and their cross sections were imaged using SEM. The cross section of the nanocomposite was then analyzed via EDS, the results of which are shown in Figure 3b–c. As annotated on the SEM image in Figure 3b, the thickness of the nanocomposite was measured as 4.8 μm. The average thickness of the nanocomposite, measured via stylus profilometry, was 6.9 μm with an average roughness value of 1.9 μm. The thickness measured in Figure 3c, then, falls within the average roughness of the measured film. The EDS elemental map, shown in Figure 3c, shows the distribution of iron (Fe) in the nickel (Ni) matrix. Though there does seem to be a section of the composite that is richer in iron towards the bottom of the elemental map in Figure 3c, this is still dispersed in a nickel matrix that then continues throughout the rest

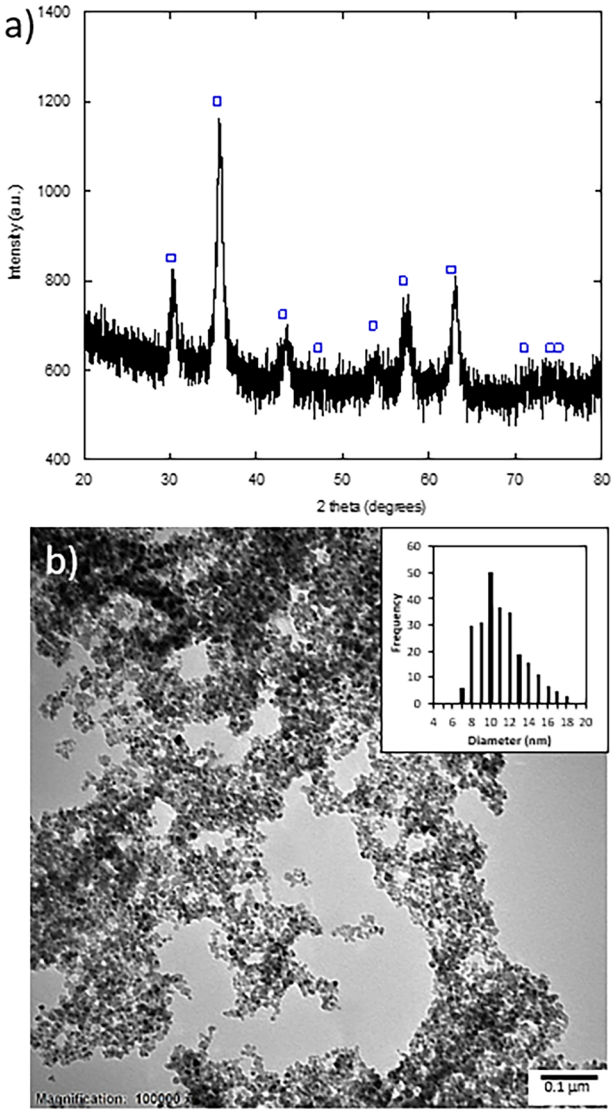

FIG. 2. X-ray diffraction (XRD) pattern (a) of the as-synthesized iron oxide nanoparticles compared to a reference magnetite pattern (98-004-4525) from the ICDD database, shown in squares. Transmission electron microscopy (TEM) image (b) of as-synthesized iron oxide nanoparticles. Distribution of sizes measured via ImageJ (n=250) shown in top right corner.

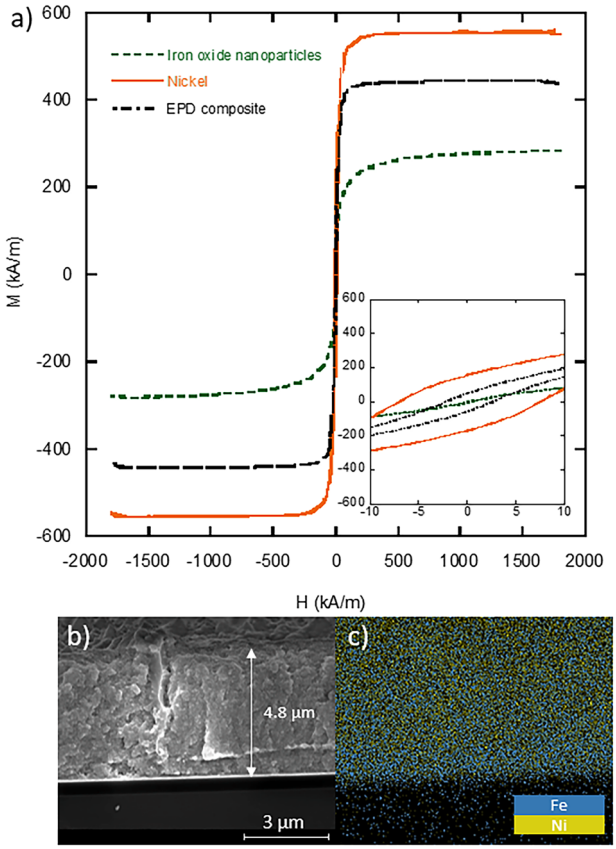

FIG. 3. Magnetization behavior obtained from vibrating sample magnetometry (VSM) (a) of the nanocomposite consisting of the electrophoretically deposited iron oxide nanoparticles. Inset in (a) shows a zoom-in to the center of the hysteresis curves. Scanning electron microscopy (SEM) (b) and electron dispersive x-ray spectroscopy (EDS) (c) images of films fabricated via EPD of iron oxide nanoparticles followed by electro-infiltration of nickel, revealing that the nanoparticles are dispersed in the nickel matrix.

of the composite. The detection of iron via EDS shows the presence of well dispersed iron oxide nanoparticles throughout the nickel matrix. This reveals that the nickel was able to infiltrate between the particles.

In order to quantify the magnetic behavior of the fabricated composites, vibrating sample magnetometry (VSM) was used. The resulting M-H curves of an iron oxide nanoparticle film, nickel-only electroplated film, and EPD composite are shown in Figure 3a. The magnetic saturation value of the nanocomposite fabricated using EPD (473 kA/m) falls between that of the iron oxide nanoparticles (280 kA/m) and electroplated nickel (555 kA/m). This indicates that the fabricated nanocomposite exhibits the desired magnetic properties that are an average of the two constituent materials. This behavior has been reported previously for magnetic nanocomposites of similar composition.[5,6,15] These results confirm the successful infiltration of nickel through the porous iron oxide nanoparticle film, thus showing the potential of combining EPD with electro-infiltration as a way for fabricating thick magnetic nanocomposites.

IV. CONCLUSION

Iron oxide nanoparticles were synthesized via co-precipitation to be used for the low loss magnetic phase for the iron oxide nanoparticle/nickel magnetic nanocomposites. These nanocomposites were fabricated via electrophoretic deposition (EPD) of the iron oxide nanoparticles into a mold and the electro-infiltration of a high magnetic saturation magnetic phase, nickel, through the porous

deposited iron oxide nanoparticle film. The fabricated nanocomposites exhibited a magnetic saturation of 473 kA/m, which fell between the magnetic saturation values of the two constituent materials, iron oxide nanoparticles and nickel. These results show the promise of electrophoretic deposition as a versatile method for fabricating thick magnetic nanocomposites for on-chip power components.

ACKNOWLEDGMENTS

The authors would like to sincerely thank the Research Service Center (RSC) staff at the University of Florida for their assistance in the fabrication and characterization of these materials. This work was funded, in part, through the National Science Foundation (CMMI-1727930).

REFERENCES

[1]Y. M. Nguyen, D. Bourrier, S. Charlot, Z. Valdez-Nava, V. Bley, C. Combettes, T. Lopez, J. Laur, and M. Brunet, J. Micromech. Microeng. **24**, 104003 (2014).
[2]S. Mathuna, T. O'Donnell, N. Wang, and K. Rinne, IEEE Trans. Power Electron. **20**, 585 (2005).
[3]P. M. Raj, P. Charkrborti, H. Sharma, K. Han, S. Gandhi, S. Sitaraman, M. Swaminathan, and R. Tummala, in Proc. IEEE, 27 (2014).
[4]K. Gorecki and K. Detka, Energies **12**, 1991 (2019).
[5]X. Wen, S. J. Kelly, J. Andrew, and D. Arnold, AIP Advances **6**, 056111 (2016).
[6]C. S. Smith, S. Savliwala, S. C. Mills, J. S. Andrew, C. Rinaldi, and D. P. Arnold, J. Magn. Magn. Mater. **493**, 165718 (2019).
[7]D. S. Gardner, G. Schrom, F. Paillet, B. Jamieson, T. Karnik, and S. Borkar, IEEE Trans. Magn. **45**, 4760 (2009).
[8]P. M. Raj, H. Sharma, S. Samtani, D. Mishra, V. Nair, and R. Tummala, J. Mater. Sci.: Mater. Electron. **24**, 3448 (2013).
[9]H. Li, D. Buesen, R. Williams, J. Henig, S. Stapf, K. Mukherjee, E. Freier, W. Lubitz, M. Winkler, T. Happe, and N. Plumere, Chem. Sci. **9**, 7596 (2018).
[10]S. Kelly, X. Wen, D. P. Arnold, and J. S. Andrew, AIP Advances **6**, 056105 (2016).
[11]L. Besra and M. Liu, Prog. Mater. Sci. **52**, 1 (2007).
[12]S. Hashi, S. Yabukami, A. Maeda, N. Takada, S. Yanase, and Y. Okazaki, J. Magn. Magn. Materials **316**, 465 (2007).
[13]S. Oberdick and S. A. Majetich, J. Phys. Chem. C **117**, 18709 (2013).
[14]S. K. Kurinec, N. Okeke, S. K. Gupta, H. Zhang, and T. D. Xiao, J. Mater. Sci. **41**, 8181 (2006).
[15]X. Wen, J. D. Starr, J. Andrew, and D. Arnold, J. Micromech. Microeng. **24**, 107001 (2014).
[16]X. Wen, J. Andrew, and D. Arnold, AIP Advances **7**, 056225 (2017).
[17]R. Massart, IEEE Trans. Magn. **17**, 1247 (1981).
[18]Q. Li, C. W. Kartikowati, S. Horie, T. Ogi, and K. Okuyama, Sci. Rep. **7**, 9894 (2017).